Thermotropic Mesomorphic Behavior of Surfactant-Encapsulated Polyoxometalate Hybrids

Wen Li, Shengyan Yi, Yuqing Wu, and Lixin Wu*

Key Laboratory for Supramolecular Structure and Materials of Ministry of Education, Jilin University, Changchun 130012, P. R. of China

Received: April 3, 2006; In Final Form: July 7, 2006

We investigate in detail novel organic−inorganic hybrid liquid crystalline materials, the complexes of surfactant-encapsulated polyoxometalate clusters (SECs), using thermal, X-ray diffraction, and FT-IR spectroscopic analyses. The differential scanning calorimetry measurements reveal four phase transitions under heating processes. We employ FT-IR spectroscopy to understand these phase behaviors. On the basis of vibration spectral assignments, the evidence suggests that the first two phase transitions are associated with the increase of gauche conformers and the disruption of alkyl chains packing in the heating run; the third phase transition is due to the full conformational disorder of alkyl chains covered on the polyoxometalates (PMs); no significant C−H stretching or wagging vibrations are observed with the fourth transition. We find that the fourth endothermic peak is sensitive to the charges of the PMs, and the transition temperature decreases from 185, 177, to 164 °C with decreasing PM charges from 13, 11, to 9, respectively. Interestingly, the temperatures of the first three phase transitions of SECs are essentially independent of the PM charges.

Introduction

Polyoxometalates (PMs) are important nanosized inorganic materials with a rich number of chemical structures and properties including uses in catalysis, medicine, optics, electronics, and magnetics.[1−3] However, applying these inorganic clusters to functional devices and materials remains a challenge because of their poor processibility. An effective strategy is to introduce PMs into amphiphilic matrixes by ion-exchange reactions; i.e., the cationic surfactants can replace the PMs' surface counterions, forming surfactant-encapsulated clusters (SECs).[4−7] Not only is the solubility of PMs promoted in regular organic solvents, but also well-ordered thin films can be easily prepared by solvent-casting and LB techniques.[8−10] Furthermore, some inherent properties of PMs are directly associated with their aggregated structures in various assemblies.[7,8,11] Previous results suggest the possibility of tuning the functional features of PM-based hybrids by the appropriate choice of organic constituent at the molecular level. Organic liquid crystals (LC) are fascinating functional materials, which can automatically self-assemble into various mesophases through organized packing of organic molecules in a certain temperature range and provide added features such as the capacity to respond to external stimuli.[12,13] It seems particularly significant to incorporate PMs into LC matrixes by employing electrostatic interaction; hybridization of PMs with LC molecules can result in novel metallomesogens, which has recently attracted a great deal of attention.[14−17] Additionally, the manifold properties of PMs may be tuned conveniently in various mesophases.

In an earlier paper, we prepared a mesomorphic cationic surfactant di[12-(4′-octyloxy-4-azophenyl)dodecyloxy]dimethylamonium bromide (L1), and polyoxometalate $K_{13}[Tb(SiW_{11}O_{39})_2]\cdot 15H_2O$ (PM-1) was embedded into the mesomorphic surfactant matrixes, forming a surfactant-encapsulated cluster $(L1)_{13}[Tb(SiW_{11}O_{39})_2]\cdot 30H_2O$ (SEC-1).[18] The hybrid exhibits thermotropic liquid-crystalline behavior, and we previously identified its mesogenic character.[18] One of our persistent interests is concentrated on the relationship between aggregated structures (or molecular level dynamics) and the properties of PMs based on the possibility of manipulating specific material properties by controlling various structures. Therefore, it is necessary to understand the phase behavior and the chain conformational dynamics of the LC complex. In this report, differential scanning calorimetry (DSC), X-ray diffraction, and FT-IR spectroscopy were employed to examine the phase behaviors of SEC-1. Some detailed results of the phase transitions were obtained concerning the conformational change of the alkyl chains. In addition, we chose two PMs: $K_{11}[Eu(PW_{11}O_{39})_2]\cdot 13H_2O$ (PM-2)[19] and $Na_9[EuW_{10}O_{36}]\cdot 32H_2O$ (PM-3)[20] to prepare two different surfactant-encapsulated PMs: $(L1)_{11}[Eu(PW_{11}O_{39})_2]\cdot 13H_2O$ (SEC-2) and $(L1)_9[EuW_{10}O_{36}]\cdot 9H_2O$ (SEC-3), respectively, bearing a core−shell ellipsoid as schematically drawn in Figure 1. We also systematically investigate the influence of PM charge on the phase behaviors of SECs.

Experimental Section

Materials Preparation. Cationic surfactant L1, $K_{13}Tb(SiW_{11}O_{39})_2\cdot 15H_2O$ (PM-1), and SEC-1 were synthesized previously.[18] $K_{11}[Eu(PW_{11}O_{39})_2]\cdot 13H_2O$ (PM-2) and $Na_9EuW_{10}O_{36}\cdot 32H_2O$ (PM-3) were prepared according to the reported literature.[20,21]

SEC-2 was synthesized using the reported procedure: PM-2 was dissolved in aqueous solution (pH = 5.7), and then L1 in chloroform solution was added stepwise. The mixture was stirred for 4 h at 40 °C. The initial molar ratio of L1 to PM-2 was controlled at 9:1. The organic phase was separated, and the complex was obtained by evaporating chloroform to dryness. Then, the sample was further dried in a vacuum until the weight remained constant. Anal. Calcd for SEC-2 ($C_{726}H_{1170}N_{55}O_{135}W_{22}EuP$, 17087.74): C, 51.03; H, 6.90; N, 4.51. Found: C, 51.48; H, 6.77; N, 4.39. Thermogravimetric analysis (TGA) suggests a mass loss of 1.38% from 30 to 100 °C arising from crystal water in SEC-2. Combining the TGA and elemental analysis,

* To whom correspondence should be addressed. E-mail: wulx@jlu.edu.cn.

10.1021/jp062074o CCC: $33.50
Published on Web 08/04/2006

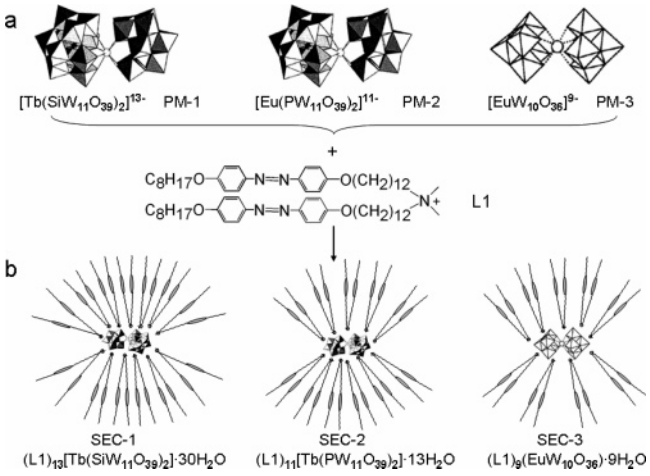

Figure 1. (a) Coordination polyhedral representations of PM-1, PM-2, and PM-3; (b) the schematic drawing of the chemical structures of SEC-1, SEC-2, and SEC-3.

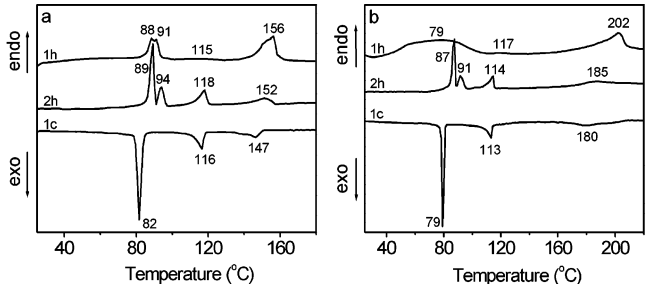

Figure 2. DSC curves of surfactant L1 (a) and SEC-1 (b) on their heating and cooling cycles (1h, the first heating; 2h, the second heating; 1c, the first cooling.).

SEC-2 should correspond to the following formula: $(L1)_{11}[Eu(PW_{11}O_{39})_2]\cdot 13H_2O$ (17087.74).

The complex SEC-3 was prepared similarly to SEC-2 by using PM-3 instead of PM-2. The initial molar ratio of L1 to PM-3 was maintained at 8:1. Anal. Calcd for SEC-3 ($C_{594}H_{954}N_{45}O_{81}W_{10}Eu$, 12012.55): C, 59.40; H, 8.00; N, 5.25. Found: C, 59.84; H, 8.37; N, 5.09. TGA suggests a mass loss of 1.34% from 30 to 110 °C arising from crystal water in SEC-3. Combining the TGA and elemental analysis, SEC-3 should correspond to the following formula: $(L1)_9EuW_{10}O_{36}\cdot 9H_2O$ (12012.55).

Measurements. Elemental analysis (C, H, N) was performed on a Flash EA1112 from ThermoQuest Italia S.P.A. Temperature-dependent infrared spectra were performed on a Bruker IFS66V Fourier transform infrared spectrometer, equipped with a DTGS detector with a resolution of 4 cm^{-1}, from pressed KBr pellets. The heating rate was 5 K/min over the temperature range 30−230 °C. TGA was conducted with a Perkin-Elmer TG/DTA-7 instrument, and the heating rate was 10 K/min. Differential scanning calorimetry (DSC) measurements were performed on a Netzsch DSC 204. The scanning rate was 5 K/min, the samples were sealed in aluminum capsules in air, and the holder atmosphere was dry nitrogen. Variable-temperature X-ray diffraction (XRD) experiments were carried out on a Rigaku X-ray diffractometer (D/max 2500V, using Cu $K\alpha_1$ radiation of a wavelength of 1.54 Å) with a PTC-20A temperature controller.

Results and Disscusion

Thermal Studies. Figure 2 displays DSC curves of surfactant L1 and complex SEC-1 in their heating and cooling cycles. We note that the first heating curves of L1 and SEC-1 are different from their second heating traces. The original samples obtained by evaporating solvent from their organic solution have different thermal behavior as compared to the samples obtained by crystallization from the melting state. This means that the thermal behavior of L1 and SEC-1 strongly depends on their thermal history. Additionally, TGA analysis of SEC-1 reveals that crystalline water is lost during the first heating process and no obvious degradation occurs below 280 °C. Therefore, in the second heating run, the crystalline water was no longer present and the DSC thermograms should illustrate the intrinsic thermal property of the employed samples after eliminating the thermal history. During the second heating run, SEC-1 clearly exhibits four phase transitions at 87, 91, 114, and 185 °C. Upon cooling, three phase transitions occur at 180, 113, and 79 °C. The hysteresis is observed in cooling process for both L1 and SEC-1. Earlier, we reported[18] that the first two endothermic peaks of SEC-1 correspond to a transition from a solid to a layered mesophase with large enthalpies $\Delta H = 229.3$ kJ/mol; the peak at 114 °C is attributed to the transition between different lamellar mesophases with $\Delta H = 69.4$ kJ/mol; the broad peak at 185 °C corresponds to the transition from the LC phase to an isotropic liquid with $\Delta H = 105$ kJ/mol.

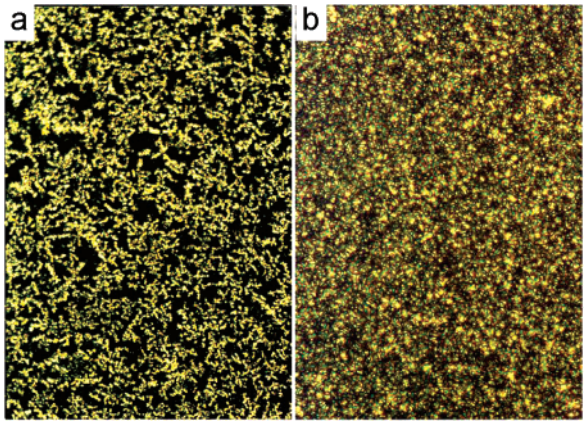

Figure 3. Optical textures of SEC-1: (a) at 103 °C, (b) at 160 °C (400×).

Polarizing optical microscopy measurements identified the LC phases of SEC-1, as shown in Figure 3. Here, grain texture was observed at 103 °C, and another similar but clear mesophase texture was seen at 160 °C during the heating process. In addition, the viscosity of SEC-1 in its mesophase is much greater than that of the surfactant L1. Taking into account the molecular weight (19458.71), we propose that the thermal property of SEC-1 is quite similar to that of LC polymers. Comparing with L1, SEC-1 exhibits mesogenic characteristics in the heating process as follows: (i) The first three phase transitions of SEC-1 are quite similar to those of L1 except that the transition temperatures are slightly lower. This implies that the thermotropic property of L1 at low temperature is maintained in SEC-1 and basically not affected by the encapsulation on the inorganic core. We earlier reported that the surfactant L1 exists in its lamellar structure.[18] In the case of SEC-1, the PM-1 is oval and we propose that most of surfactants align along its long axis, which is favorable for ordered and oriented packing in self-assembly lamellar structures.[18] Therefore, we suggest that the aggregated manner of L1 in SEC-1 is similar to that of the original surfactant in the low-temperature region. We propose that the slight decrease of the transition temperature for SEC-1 arises from the curvature of the ellipsoid structure of PM-1. (ii) The transition temperature of SEC-1 at the clearing point increases

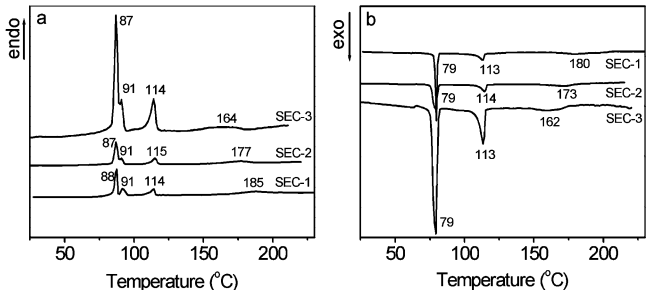

Figure 4. DSC curves of SECs: (a) second heating; (b) first cooling.

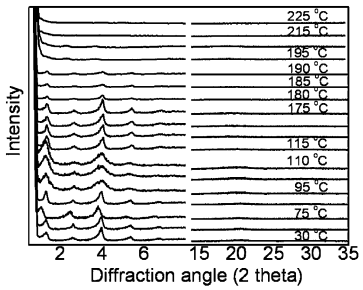

Figure 5. Variable-temperature X-ray diffraction of SEC-1.

markedly and the peak becomes broad in comparison with the corresponding transition of L1. This distinct difference indicates the mesophase of SEC-1 is more stable than that of L1, which implies that the transition is correlated with the strongly electrostatic interaction between the cationic surfactant L1 and the anionic PM-1. The charges of PMs will affect the phase transition temperature of SEC-1.

Such speculation is further supported by examining the thermal properties of SEC-2 and SEC-3, as shown in Figure 4. Similar to SEC-1, the DSC curves of SEC-2 and SEC-3 clearly exhibit four endothermic transitions with the heating process and three exothermic transitions with the cooling process. It is interesting that the temperatures of the first three endothermic peaks and two exothermic peaks for the low-temperature region in all three complexes are nearly uniform. We therefore conclude that all the complexes possess identical structures and their phase transition temperatures for the low-temperature region are independent of the PMs' charge number. This indicates that the phase transitions occurring in the low-temperature region are derived from the thermal changes of surfactant molecules in SECs. In addition, PM-1, PM-2, and PM-3 possess almost the same size and elliptical structure except for the difference in charge number.[11,19,20] The charge difference of PMs is regularly reflected in the clearing points of SECs, which decrease markedly from 185, 177, to 164 °C with decreasing the charged numbers of PMs from 13, 11, to 9. This suggests that the ability to stabilize the mesophase corresponds to the following trend: the higher the charge of PM, the more stable the mesophase. The alkyl chain length of surfactants has no apparent influence on the clearing point (the details will be discussed in future work). Our evidence indicates that the strong electrostatic forces are favorable for stabilizing the mesophases of SECs, which results in an increase of the transition temperature at the clearing point.

We further investigate the mesophases of SEC-1 by temperature-dependent X-ray diffraction, and the results are shown in Figure 5. SEC-1 displays layered structures in its solid and LC phases with five equidistant peaks in the low-angle region of the diffraction pattern. We previously presented that the mesophase sequence of SEC-1 in the cooling process is I−SmX_1−SmX_2−Solid, and in the LC phase the alkyl chains of surfactants are partially interdigitated and/or tilted with respect to the layer normal.[18] It can be seen from Figure 5 that the layer spacing of SEC-1 increases on transforming from the solid state to SmX_2 in the heating run and decreases gradually with increasing temperature. In fact, the solid phase of SEC-1 is most likely to be biaxial with alkyl chains tilted with respect to the layer normal. The layer spacing of SEC-1 increases on transforming from the solid state to SmX_2, which indicates that the structure undergoes a conformational change of alkyl chains and decreasing angle of tilt with respect to the layer normal. When SEC-1 transforms from SmX_2−SmX_1 with temperature, an increase in the frequency of gauche bends shortens the distance between an ammonium headgroup and a methyl chain terminus, thereby decreasing the layer spacing. At clearing point, the lamellar structure of SEC-1 is maintained in a large temperature range of 175−190 °C. This means the transition of SEC-1 from LC state to an isotropic liquid does not occur under a sudden temperature change but is rather a slow process. This result is consistent with the broad band at the clearing point observed from DSC curves of the SEC-1 (Figure 4). We therefore reasonably conclude that the broad peak at the clearing point is a result of the strong electrostatic interactions between the ammonium headgroups and the PM-1.

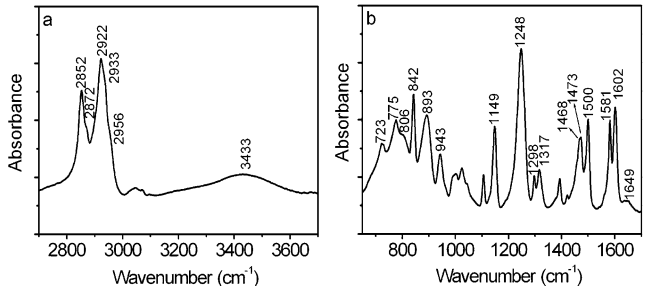

Figure 6. IR spectrum of virgin SEC-1 at room temperature: (a) high-frequency region (2700−3700 cm^{-1}) and (b) low-frequency region (650−1700 cm^{-1}).

FT-IR Spectrum of SEC-1 at Room Temperature. Fourier transform infrared (FT-IR) spectroscopy provides a highly sensitive probe of molecular structure and dynamics of alkyl chains.[22,23] As shown in Figure 6, a broad band at 3433 cm^{-1}, assigned to the O−H stretching mode, indicates the presence of crystalline water in SEC-1. The water molecules can be removed under heating, which is in consistent with the result of TGA.[18] Two weak but distinct bands observed at 2956 and 2872 cm^{-1} are assigned to antisymmetric (r^-) and symmetric (r^+) stretching vibrations of the terminal methyl groups, respectively. Additionally, we observe a shoulder peak at 2933 cm^{-1}, which is attributed to Fermi resonances absorption due to r^+ mode; this is indicative of the zigzag conformer of the hydrocarbon chain of SEC-1.[24] We assign the bands at 2922 and 2852 cm^{-1} to antisymmetric (d^-) and symmetric (d^+) stretching vibrations of the methylene group, respectively. It is well appreciated that d^- and d^+ bands are strong indicators of the chain conformation: low wavenumbers (2915−2918 and 2846−2850 cm^{-1}) of the bands are characteristic of highly ordered alkyl chains,[25,26] while their upward shifts (2924−2928 and 2854−2856 cm^{-1}) are indicative of the increase in gauche conformers, implying the alkyl chain conformation tends toward disorder. On the basis of this rule, the observed frequencies of 2922 and 2852 cm^{-1} for SEC-1 at room temperature indicate the presence of gauche conformers of alkyl chains. In the lower frequency region as shown in Figure 6b, a weak band is observed at 1649 cm^{-1}, belonging to the bending mode of water molecules. The aromatic

ring vibration modes are located at 1602, 1581, and 1500 cm^{-1}.[27] The slightly split peaks at 1473 and 1468 cm^{-1} are associated with CH_2 scissoring bending modes, which are widely used to diagnose alkyl chains packing.[28,29] The appearance of a single narrow peak at 1473 cm^{-1} is attributed to triclinic subcell packing of alkyl chains, and the single narrow band at 1467 cm^{-1} corresponds to hexagonal subcell. The appearance of the well-resolved doublet with two distinct components is known to either derive from intermolecular vibrational coupling because of crystal-field splitting in orthorhombic/monoclinic packing or from the coexistence of triclinic and hexagonal packing in solid state. In the present case, the less resolved doublet is possibly derived from the latter because the packing of the alkyl chains is not close as can be elucidated by their frequencies at high-wavenumber region. The band at 1394 cm^{-1} corresponds to CH_3-N^+ scissoring bending mode.[30,31] The strong band at 1248 cm^{-1} is due to the phenyl ring−O vibration mode.[32] The weak bands at 1317 and 1298 cm^{-1} are assigned to CH_2 wagging modes. The band located at 1149 cm^{-1} is associated with phenyl−N stretching mode.[33] We assign the less intensity vibration in the region 1000−1120 cm^{-1} to the ring deformation modes. The band at 943 cm^{-1} arises from W−Od antisymmetric stretching. The bands at 893 and 842 cm^{-1} are attributed to a W−Ob antisymmetric stretching,[34] and out-of-plane deformation of the phenyl ring,[35] respectively. Those bands at 806 and 775 cm^{-1} are due to W−Oc antisymmetric and symmetric stretching modes, respectively.[34] In addition, the band at 723 cm^{-1} is characteristic of the methylene C−H rocking mode in an alkyl chain with $CH-(CH_2)_n$ ($n \geq 4$).[36]

Temperature-Dependent FT-IR Spectra of SEC-1. In the range of 25−230 °C, the infrared spectra of SEC-1 that has eliminated thermal history, at high wavenumbers, are shown in Supporting Information (Figure S1a). The Fermi resonance absorption band that emerged at 2933 cm^{-1} disappears when the temperature rises to 80−95 °C, indicative of increasing disorder of the packed alkyl chains. To further analyze the temperature dependence of packed alkyl-chain structure, we quantify the frequency changes of d^- and d^+ as a function of the temperature in Figure 7a. The initial plateau at 2922 cm^{-1} is retained until 80 °C, suggesting little change in the d^- conformation in this temperature region. An obvious shift of the methylene antisymmetric stretching mode to higher wavenumbers is observed in the temperature range of 80−95 °C, which also corresponds to the first and second phase transitions observed from our DSC measurements. The absorption band shift clearly illustrates an increasing accumulation of gauche conformers in the alkyl chain ensembles, and subsequently reaching an abrupt phase transition. The new plateau at 2924 cm^{-1} is kept from 95 to 110 °C, suggesting that the alkyl chains are quite disordered. Whereas the wavenumber keeps slightly lower than the reported typical value for complete disordered conformation,[37] it does not move to 2926 cm^{-1} until the following phase transition occurs between 110 and 120 °C, which corresponds to the third phase transition given by our DSC measurements. The symmetric stretching mode of methylene appears not very sensitive to the aggregated structural change as its wavenumber remains constant from 25 to 110 °C through the first and second phase transitions, as shown in Figure 7b. We observe an obvious band shift from 2852 to 2854 cm^{-1} in the temperature range of 110 to 120 °C, which is in good agreement with the third phase transition. Thereafter, the band position keeps unchanged until the temperature reaches the clearing point, implying the existence of disordered alkyl chains similar to that found in molecular liquid.[38]

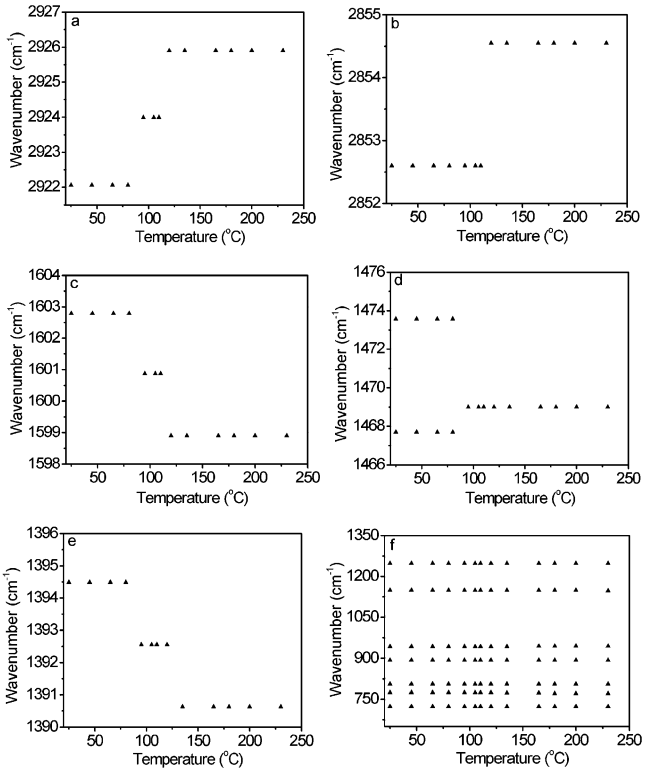

Figure 7. Temperature dependence of the positions of IR bands of SEC-1: (a) antisymmetric CH_2 stretching mode, (b) symmetric CH_2 stretching mode, (c) aromatic ring vibration mode, (d) CH_2 scissoring mode, (e) CH_3-N^+ scissoring mode, and (f) CH_2 wagging mode and PM-1 vibration mode.

The temperature-dependent infrared spectra in the range of 1350−1680 cm^{-1} are shown in Figure S1b, from which many changes involving the vibrations of alkyl chains and phenyl ring are observed. The vibration band assigned to phenyl ring shifts from 1603 to 1599 cm^{-1} after a short plateau at 1601 cm^{-1} when the temperature rises from 80 to 120 °C as summarized in Figure 7c. Meanwhile, the intensity ratio of 1581 cm^{-1} to 1602 cm^{-1}, from which we can estimate the change of azobenzene group, shows a visible decrease from 80 to 120 °C (Figure S2). The data demonstrates the change of the azobenzene unit with temperature, but it is difficult to provide powerful proof about the detailed phase behavior of the azobenzene unit because we cannot find the detailed information regarding the orientation change based on temperature-dependent IR spectra.

The methylene scissoring modes display sensitive change with temperature (Figure 7d). The less split bands at 1473 and 1468 cm^{-1} combine into a single peak at 1469 cm^{-1} in the temperature range between 80 and 95 °C. Taking into account the shift in frequency and the observed broadening of this band, we associate the main structural transition with the disruption of the lateral packing arrangement of the alkyl chains around the first two transitions. The band at 1394 cm^{-1} also shows two discontinuous changes (Figure 7e) at 80−95 °C and 140−160 °C. The evidence points to changes in the disposition of the ammonium headgroups.

The vibration bands arising from PM-1 in the low-frequency region are temperature independent and remain constant up to 230 °C (Figure S1c and Figure 7f). The constant band positions indicate that the rigid inorganic core is intact and not distorted during the entire heating cycle. The spectroscopy results demonstrated that the alkyl chains of surfactants have melted completely after the first three phase transitions in the heating

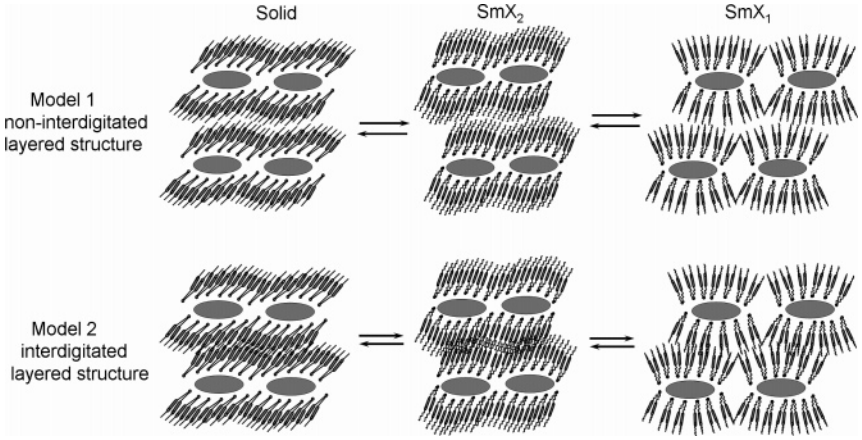

Figure 8. Schematic representations of the possible lamellar packing and structure changes of SECs with temperature.

process, and no obvious C−H stretching and wagging vibrations are observed at the clearing point.

Conclusions

By encapsulating PMs with surfactants bearing azobenzene groups we obtain novel hybrid LC materials. The combined LC materials bring forth interesting self-assembling and phase behaviors. Under heating, all SEC-1, SEC-2, and SEC-3 exhibit four phase transitions. The first two phase transitions correspond to an increase of gauche conformers of the alkyl chains and the following disruption of the alkyl chain packing. The third transition arises from the complete conformational disorder of the alkyl chains. The transition at clearing point does not have a clear signature in the change of C−H stretching or wagging vibrations. This means that in the liquid-crystalline state, even after the alkyl chains have melted completely, the electrostatic interaction between cationic heads and PMs remain unbroken and free molecular motion of the surfactants is prevented by the rigidity of the ionic layers. Possible packing structures of SEC-1 are shown in Figure 8. The PM-1 remains intact and is not distorted during the heating process. The first three phase transitions of the three SECs occur at almost the same temperatures, and are accompanied by sharp changes of the C−H stretching and CH_2 scissoring modes as well as of the phenyl rings. This result, together with their similarities to those phase transitions of L1, proves that structural changes of SECs start from outside alkyl chains covered on the inorganic core, and the arrangement of surfactant molecules in SECs should be in agreement with that of neat L1. In addition, the phase behaviors of SECs in the low-temperature region are independent of the PMs' charges. The transition temperatures of SECs at the clearing point increase with increasing charge numbers of PMs. The fact suggests that the transition temperature at the clearing point can be controlled by adjusting the charge numbers of PMs. Furthermore, introduction of PMs into the LC surfactant matrix can strengthen the thermodynamic stability of the SEC layered structure. We believe that thermal investigation of these systems will improve our knowledge about mechanisms of self-assembly, temperature-dependent phase behavior, and chain dynamics of PM-based hybrid LC materials.

Acknowledgment. This work was financially supported by the National Natural Science Foundation of China (Grant 20473032), PCSIRT of Ministry of Education of China (IRT0422), Innovation Fund of Jilin University, and the Open Project of State Key Laboratory of Polymer Physics and Chemistry of CAS. We appreciate Dr. J. Lewis from West Virginia University for his kind English corrections on the occasion of visiting us.

Supporting Information Available: Figures showing temperature-dependent IR spectra of SEC-1 and the intensity ratio of 1581 cm^{-1} to 1602 cm^{-1} with temperature. This material is available free of charge via the Internet at http://pubs.acs.org.

References and Notes

(1) Pope, M. T.; Müller, A. *Angew. Chem., Int. Ed. Engl.* **1991**, *30*, 34.
(2) Hill, C. L.; Prosser-McCartha, C. M. *Coord. Chem. Rev.* **1995**, *143*, 407.
(3) Hill, C. L. *Chem. Rev.* **1998**, *98*, the entire issue.
(4) Kurth, D. G.; Lehmann, P.; Volkmer, D.; Cölfen, H.; Koop, M. J.; Müller, A.; Du Chesne, A. *Chem.-Eur. J.* **2000**, *6*, 385.
(5) Volkmer, D.; Du Chesne, A.; Kurth, D. G.; Schnablegger, H.; Lehmann, P.; Koop, M. J.; Müller, A. *J. Am. Chem. Soc.* **2000**, *122*, 1995.
(6) Bu, W.; Fan, H.; Wu, L.; Hou, X.; Hu, C.; Zhang, G.; Zhang, X. *Langmuir* **2002**, *18*, 6398.
(7) Bu, W.; Wu, L.; Zhang, X.; Tang, A.-C. *J. Phys. Chem. B* **2003**, *107*, 13425.
(8) Zhang, T.; Spitz, C.; Antonietti, M.; Faul Charl, F. J. *Chem.-Eur. J.* **2005**, *11*, 1001.
(9) Bu, W.; Li, H.; Sun, H.; Yin S.; Wu, L. *J. Am. Chem. Soc.* **2005**, *127*, 8016.
(10) Li, H.; Qi, W.; Li, W.; Bu, W.; Wu, L. *Adv. Mater.* **2005**, *17*, 2688.
(11) Bu, W.; Li, H.; Li, W.; Wu, L.; Zhai, C.; Wu, Y. *J. Phys. Chem. B* **2004**, *108*, 12776.
(12) Demus, D.; Goodby, J.; Gray, G. W.; Spiess, H.-W.; Vill, V. *Handbook of Liquid Crystals*; Wiley-VCH: Weinheim, Germany, 1998.
(13) Tschierske, C. *J. Mater. Chem.* **1998**, *8*, 1485.
(14) Binnemans, K.; Görller-Walrand, C. *Chem. Rev.* **2002**, *102*, 2303.
(15) Donnio, B.; Guillon, D.; Deschenaux, R.; Bruce, D. W. *Comprehensive Coordination Chemistry II*; Elsevier: Oxford, 2003; Vol. 7, Chapter 7.9.
(16) Hudson, S. A.; Maitlis, P. M. *Chem. Rev.* **1993**, *93*, 861.
(17) Serrano, J. L. *Metallomesogens, Synthesis, Properties and Applications*; Wiley-VCH: Weinheim, Germany, 1996.
(18) Li, W.; Bu, W.; Li, H.; Wu, L.; Li, M. *Chem. Commun.* **2005**, 3785 and supplementary information.
(19) Tourné, C. M.; Tourné, G. F.; Brianso, M. C. *Acta Crystallogr.* **1980**, *B36*, 2012.
(20) Yamase, T.; Sugeta, M. *Bull. Chem. Soc. Jpn.* **1993**, *66*, 444.
(21) Peacock, R. D.; Weakley, T. J. R. *J. Chem. Soc. A.* **1971**, 1836.
(22) Casal, H. L.; Cameron, D. G.; Mantsch, H. H. *J. Phys. Chem.* **1985**, *89*, 5557.
(23) Almirrante, C.; Minoni, G.; Zerbi, G. *J. Phys. Chem.* **1986**, *90*, 852.
(24) Snyder, R. G.; Hsu, S. L.; Krimm, S. *Spectrochim. Acta* **1978**, *34*, 395. Bardeau, J. F.; Parikh, A. N.; Beers, J. D.; Swanson, B. I. *J. Phys. Chem. B* **2000**, *104*, 627.
(25) MacPhail, R. A.; Strauss, H. L.; Snyder, R. G.; Elliger, C. A. *J. Phys. Chem.* **1984**, *88*, 334.

(26) Wang, Q.; Zhao, B.; Zhang, X.; Shen, J and Ozaki, Y. *Langmuir* **2002**, *18*, 9845.
(27) Taniike, K.; Matsumoto, T.; Sato, T.; Ozaki, Y**.** *J. Phys. Chem.* **1996**, *100*, 15508.
(28) Hagemann, H.; Snyder, R. G.; Peacock, A. J.; Mandelkern, L. *Macromolecules* **1989**, *22*, 3600.
(29) Borja, M.; Dutta, P. K. *J. Phys. Chem*. **1992**, *96*, 5434.
(30) Scheuing, D. R.; Weers, J. G. *Langmuir* **1990,** *6***,** 665.
(31) Sikirić, M.; Šmit, I.; Tušek-Božić, L.; Tomašić, V.; Pucić, I.; Primožić, I.; Filipović-Vinceković, N. *Langmuir* **2003**, *19*, 10044.
(32) Tao, Y. T.; Lee, M. T.; Chang, S. C. *J. Am. Chem. Soc.* **1993**, *115*, 9547.
(33) Wang, R.; Yang, J.; Wang, H.; Tang, D. X.; Jiang, L.; Li, T. J. *Thin Solid Films* **1995**, *256*, 205.
(34) Rocchoccioli-Deltcheff, C.; Fournier, M.; Franck, R.; Thouvenot, R. *Inorg. Chem*. **1983**, *22*, 207.
(35) Taniike, K.; Matsumoto, T.; Sato, T.; Ozaki, Y**.** *J. Phys. Chem.* **1996**, *100*, 15508.
(36) Snyder, R. G. *J. Chem. Phys*. **1967**, *47* (4), 1316. Tyagi, O. S.; Bisht, H. S.; Chatterjee, A. K. *J. Phys. Chem. B* **2004**, *108*, 3010.
(37) Snyder, R. G.; Strauss, H. L.; Elliger, C. A. *J. Phys. Chem.* **1982**, *86*, 5145.
(38) Dorset, D. L.; Strauss, H. L.; Snyder, R. G. *J. Phys. Chem*. **1991**, *95*, 938.